# 2D Self-Bundled CdS Nanorods with Micrometer Dimension in the Absence of an External Directing Process

**Chia-Cheng Kang,[†] Chih-Wei Lai,[†] Hsin-Chieh Peng,[†] Jing-Jong Shyue,[‡,*] and Pi-Tai Chou[†,*]**

[†]Department of Chemistry, National Taiwan University, Taipei 106, Taiwan, and [‡]Research Center for Applied Science, Academia Sinica, Taipei 115, Taiwan

**ABSTRACT** In the absence of an external direction-controlling process, exclusive self-bundled arrays of CdS nanorods are formed using a facile solution-based method involving trioctylphosphine (TOP) and tetradecylphosphonic acids (TDPA) as cosurfactants. CdS self-bundled arrays with an area of as large as 2.0 $\mu m^2$ could be obtained. A detailed mechanistic investigation leads us to conclude that the matching in nanorod concentration, intrinsic properties of CdS, and the hydrocarbon chains of the surfactants between adjacent CdS rods play key roles in the self-assembly. In sharp contrast to the defect dominant emission in solutions, the self-bundled CdS nanorods exhibit optical emission nearly free from the defect-states, demonstrating their potential for applications in luminescence and photovoltaic devices.

**KEYWORDS:** CdS · nanorod · self-assembly · semiconductor · nanocrystal



In addition to zero dimensional semiconductor nanoparticles (also referred to as "quantum dots"), one-dimensional semiconductor nanocrystals that are several nanometers in diameter and have different aspect ratios have also drawn much attention because of their fascinating size-dependent optical and electronic properties. Pioneering works have unravelled unique linear polarized emission along the *c*-axis of crystals in CdSe and CdSe/CdS (core/shell) nanorods owing to their intrinsic dipolar structure.[1–5] Concurrently, tremendous efforts have been devoted to the alternative synthesizing routes and the growth mechanism of semiconductor nanocrystals.[6–22] Regarding the updated progress, the Gibbs−Curie−Wulff theorem, which concludes that minimization of total free energy in the reaction system is essential to determine the crystalline shapes, may not be valid in explaining the anisotropic shape-controlling models of nanocrystals.[1,6–8,13,16] Alternatively, the models of effective-monomer,[1,7,8,16] selective-adsorption,[6] and the presence of "magic-sized" nuclei[7,13] turn out to be more appropriate in rationalizing the kinetic growth mechanism of the semiconducting nanorods.

Elongated semiconducting nanocrystals, such as CdSe or CdTe nanorods, are highly attractive for photovoltaic applications due to their ability to transport charges along the long axis.[23,24] Nowadays, state-of-the-art synthetic techniques can provide nanorods with uniform size and shape distribution.[6–8,11–13,19] These nanorods can also offer a route to systematically study the effect of shape on the phase behavior, namely the liquid crystalline phase and self-assembled superstructures. Moreover, macroscopic assembly of nanorods might have advantages for applications in photovoltaic, field emission, and data storage devices. Onsager first claimed that anisotropic particles may form a liquid crystalline phase, which shows long-range ordering in orientation but disordering in position.[25] Further research supports this notable theory, and large-scale spatial organization has been obtained by depositing concentrated solutions of CdSe and CdSe/CdS heterostructure aggregates onto substrates.[26–28] Recently, Alivisatos and coworkers reported the assembly of CdS nanorod superlattices by the combination of a DC electric field and controlled solvent evaporation.[29] During gentle evaporation of toluene, the CdS nanorods were confined into an array by the DC electric field, making the long axis of the rods in the same direction. The net effect was a 2D superlattice "standing" on the substrate. Concurrently, Gupta *et al.* discovered similar results with CdSe nanorods.[30] The surface of CdSe nanorods was modified by polyethylene oxide (PEO) or polystyrene (PS). Poly(methyl methacrylate) (PMMA) or poly(3-hexylthiophene) (P3HT) was added to the CdSe solution to serve as the poly-

*Address correspondence to chop@ntu.edu.tw, shyue@gate.sinica.edu.tw.

Received for review January 11, 2008 and accepted March 25, 2008.

**Published online April 5, 2008.**
10.1021/nn800020h CCC: $40.75

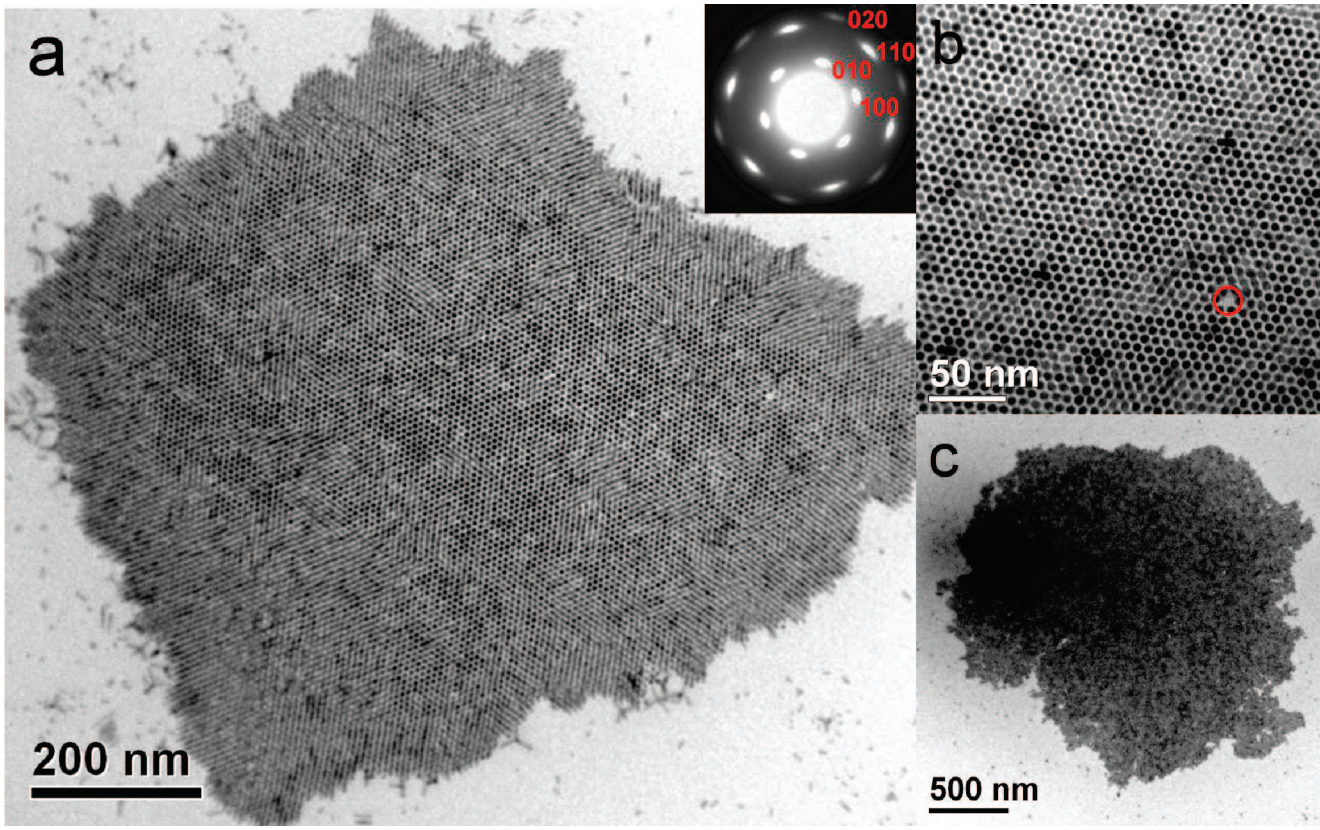


**Figure 1. (a) TEM image of TDPA- and TOP-capped CdS nanorods with self-assembled organization in large scale. The inset shows the diffraction pattern of the bundle. (b) TEM image of bundled-up CdS nanorods in higher magnification. (c) An extended TEM image of self-assembled CdS nanorods.**



mer matrix. In the presence of an electricfield, alkane-covered CdSe nanorods were corralled into densely packed arrays because of the polymer−ligand interaction. Since poly(3-hexylthiophene) is a common photoactive polymer, the polymer-nanorod assembly appears to have the potential for photovoltaic applications. In 2007, Ryan's group reported supercrystallization of CdS nanorods into perpendicular superlattices.[31] *Via* the assistance of highly oriented pyrolytic graphite (HOPG), hexagonal oriented domains of CdS nanorod bundles can be obtained on a variety of substrates without an external electric field. More recently, Manna's group synthesized CdS nanorods through a seeded-growth approach in which CdSe nanoparticles were used as seeds to produce asymmetric core−shell CdSe/CdS nanorods. By evaporating the solvent at the toluene/water interface or under the applied electric field, large areas of vertically aligned nanorods arrays were obtained.[32]

To investigate the internal force that laterally bunches nanorods together, Korgel and co-workers calculated the dipole−dipole attractive force and van der Waals attraction of self-alignment CdS nanorods.[33] The result of calculations suggested that side-by-side alignment was more favorable than the end-to-end case. Conversely, experimental results from the same report showed networks of end-to-end stripes instead of side-by-side assembly, and it was thus proposed that the formation of stripes was kinetically limited, or mediated, by solvent evaporation. Also, He *et al*. studied the self-assembly of CdSe nanorods at the oil−toluene water interface.[34] During the solvent evaporation, as the surface area of the droplet decreases, the in-plane compression and the interfacial tension play important roles in the formation of two-dimensional assembled structures.

Although the bundling of 1D semiconductor nanostructures has been theoretically predicted and experimentally observed, exclusively well-aligned arrays of nanorods without an external direction-controlling force, for example, applying an external electric field or evaporation in the presence of ordered substrate, have not been reported yet. In this work, upon capping CdS with tri-*n*-octylphosphine (TOP) and tetradecylphosphonic acid (TDPA) with the optimum ratio, exclusive formation of arrays of self-bundled CdS nanorods (~5 nm in diameter and ~15 nm in length) without the presence of an external electric field or the direction-controlling substrates was observed. It is found that as the solvent evaporates and the concentration of the solid increases, the decreasing of the interfacial energy of the nanorods caused by interlacing the alkyl chains of surfactants plays a key factor to account for the driv-

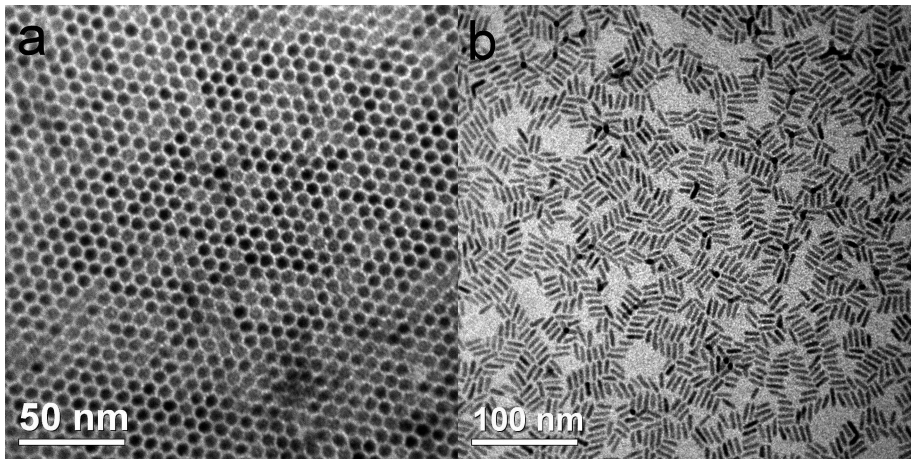


**Figure 2. TEM image of TDPA- and TOP-capped CdS nanorods with concentrations of (a) 2.5 and (b) 0.5 wt %.**

ing force. Details of the results and discussion regarding the assembled CdS nanorods are elaborated as follows.

## RESULTS AND DISCUSSION

Figure 1 panels a and b show TEM images of TDPA and TOP capped, self-assembled CdS nanorods in different scales. Evidently, as depicted in Figure 1a,b, exclusive honeycomb structures were formed. Note that the results are independent of the TEM probing area, as supported by the observation of whole self-bundled CdS nanorods in a largely extended area of micrometer dimensions depicted in Figure 1c. Because the crystal structure of CdS is wurtzite and the growing direction is along the *c*-axis, nanorods with a hexagonal cross-section are anticipated. The single-crystal-like selective-area diffraction pattern (inset in Figure 1a; note that the effective aperture size is ~100 nm and multiple nanorods in the same domain contribute to the pattern) indicates that in addition to the alignment along the *c*-axis, the basalplane (*a*- and *b*-axis) is also self-aligned. The slightly diffused diffraction spots suggest that the basalplane of the rods are rotated within 10°, similar to the results reported by Ryan's group.[31] Note Figure 1b shows nearly perfect 2D assembly, in which only one vacancy in the lower right part (marked by a red circle) is seen from the uniform hexagonal packing of the CdS nanorods perpendicular to the substrate. The intriguing issue therefore lies in the reason for the predominant corralling of the nanorods. According to previous reports about the self-assembled CdS superstructure,[29–31,34] evaporation of the solvent causes the corralling-together of the nanorods. However, without direction-controlling external interference,[34] the nanorods should form three phases of packing, namely, smectic, columnar, and crystal, due to the reduction of interfacial energy. Capillary attraction might help the formation of an ordered structure but could not force the nanorods to rearrange normal to the interface. Note that the outer edge of the bundled structure in Figure 1a shows a slight tilt of the nanorods, being depicted as a columnar structure,[34] (also see Figure S-1 in the Supporting Infromation; the Fourier filtered micrograph with enhanced contrast is presented to view the leaning behavior of edges) the result of which implies that in our experiments, evaporation-induced corralling of the nanorods might be the origin of the self-assembled CdS superstructure. On the other hand, direction-controlling processes such as external DC electric field,[29] polymer matrix,[30] and highly oriented pyrolytic carbon[31] all have the purpose of orientating the nanorods perpendicular to the substrate during gentle evaporation of solvent. However, these external direction-controlling methods are not used in this study to control the assembly behavior. As a result, besides the evaporation-induced aggregation of the nanorods, we may narrow down the discussion to the following aspects.

We first consider the concentration effect of the nanorods in the solvent. The sample shown in Figure 1 was prepared with a (toluene) solution that contains 2.5% CdS in weight. With an increase in the weight percentage from 2.5% to 5%, the same 2D assembly with an area as large as a micrometer dimension was obtained (see Figure S-2 in Supporting Information). However, as shown in Figure 2 panels a and b, with a decrease of the concentration of the CdS nanorods from 2.5 to 0.5 wt %, the 2D framework gradually collapsed. At a concentration of ~0.5 wt %, as shown in Figure 2b, a lying-down monolayer of CdS nanorods with their *c*-axis parallel to the plane of the grid was clearly observed. Therefore, it is reasonable to predict that the critical concentration of the CdS nanorods in toluene for obtaining the assembled structure might be between 0.5% and 2.5% in weight.

Nevertheless, despite the lack of a 2D framework of the CdS nanorods, judging from the TEM image shown in Figure 2b, most of the nanorods are still aligned side by side. The results imply the possible existence of the influence of the surfactants between nanorods, and surfactants that surround the CdS nanorods might play an important role in the self-bundled superstructure. Initially, the reaction system contains Cd-TDPA complex, sulfur, and TOP, among which the surfactants that affect shape and aspect ratios are ascribed to TDPA and TOP. Therefore, interaction between the alkyl groups of surfactants might serve as the direction-controlling agent. The tendency of self-association of the hydrocarbon part on the surfactant is known to be the driving force for the micelle formation. Wishnia[36]

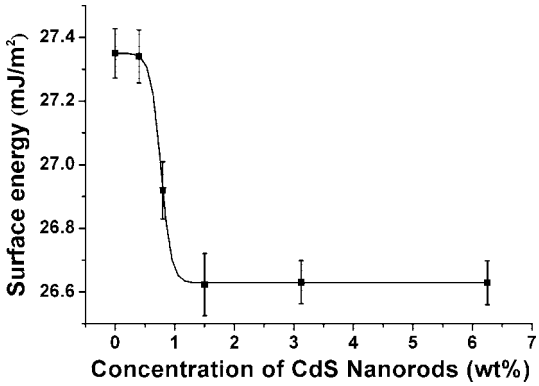


**Figure 3. The surface energy, measured by pendent drop method, with respect to different concentrations of CdS nanorods (0, 0.4, 0.8, 1.5, 3.125, and 6.25 wt %).**

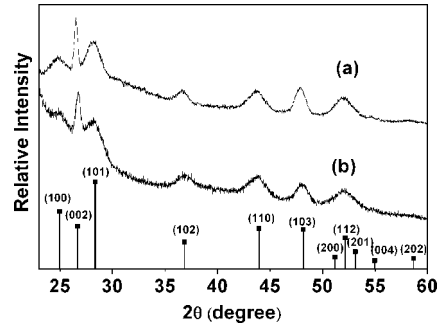


**Figure 4. Powder X-ray diffraction (XRD) of CdS nanorods synthesized by using (a) TDPA and TOP, (b) TDPA, HDA, and TOP, and that of standard CdS (wurtzite) pattern (lower).**

has measured the solubility of hydrocarbons such as ethane, propane, butane, and pentane in sodium dodecyl sulfate (SDS) solution and concluded that the hydrocarbon contribution to the standard free energy is in the range of $-12.0RT$ to $-18.2RT$. To a certain degree, the intercrossed hydrocarbon groups of TOP and TDPA that occupy the space between two neighboring CdS nanorods would reduce the free energy and help the self-assembly of CdS nanorods as well. To further manifest this viewpoint, we thus measured the surface energy of solutions containing different concentrations of CdS nanorods. As shown in Figure 3, at the interval of CdS nanorod concentration from 0.4 to 1.5 wt %, the surface energy of the solution gradually decreases as the surface concentration of the nanorod increases with the total concentration. Above 1.5 wt %, the surface energy of the solution is independent of the total concentration, indicating a constant surface concentration of the nanorod. In other words, the nanorod is saturated in the solution, and aggregates will form to minimize the energy. According to the plot depicted in Figure 3, the critical concentration of the CdS nanorods in toluene should be between 1.0% and 2.0% in weight, in good agreement with the concentration used for the TEM observation of 2D self-bundled CdS nanorods (vide supra). This variation of surface energy supports the fact that upon increasing the concentration of nanorods in the solution, CdS nanorods saturate and self-assemble into bundles.

Considering a self-assembled monolayer composed of the organic molecules with a headgroup and a long-chain alkane tail on the surface of semiconductor, Bent[37] recently concluded that the net result of competition between intermolecular and interfacial forces tends to alter the behavior of the monolayers. Good alignment of the alkane tails could be achieved in the case if intermolecular forces overcome the molecule−substrate and lattice forces. On the contrary, if the interfacial forces appear to dominate over the interchain forces, the head groups form commensurate bonding with the underlying surface. Hence, extensively ordered coverage of the head groups on the surface causes mismatch between the semiconductor lattice and molecule−molecule spacing among the head groups. This strain could be released by disordering of the alkane tails, such that the ordered packing of the alkane chains may not be available eventually. These viewpoints further support our observations in the concentration-dependent experiments of the surface energy. In other words, after the concentration of CdS nanorods reaches the critical value (0.4 wt %), the intermolecular forces among the alkane-chains of surfactants on adjacent CdS nanorods surpass the interfacial forces between the adsorbed head groups and the surface of the nanorods. Consequently, the construction of self-assembled arrays of CdS nanorods comes with a lowering of surface energy.

In addition to the solvent-evaporation induced self-assembly, the other key topic would be the direction-controlling effect of the surfactants. We further propose that the three octyl chains from one single TOP molecule might establish a stronger unidirectional superstructure than those surfactants with single hydrocarbon chains. To verify this hypothesis, we thus tentatively used hexadecylamine (HDA) to substitute part of TOP. Figure 4 shows the X-ray powder diffraction (XRD) patterns of the CdS nanorods prepared by using two sets of surfactants: (a) TDPA and TOP (molar ratio of 1:15) and (b) TDPA, HDA, and TOP (molar ratio of 1:3.5:6, see Experimental Section for details). Both patterns show the diffraction peaks matching exactly that of the wurtzite CdS standard pattern (see bottom part of Figure 4). The significantly sharp and narrowed (002) peak at 26.7 degrees (2θ) clearly supports the extended *c*-axis stacking domain of the wurtzite lattice. Note that the broadening of other peaks is due to the corresponding quantized dimensions. Figure 5 shows the TEM image of the CdS nanorods synthesized by using TDPA, HDA, and TOP as surfactants. With control of the concentration of the nanorods (2.0 wt %), self-assembly of the nanorods could also be seen on the carbon-coated copper grid. However, more than half of the nanorods in the bundle leaned on the substrate, even though the crystalline structure (XRD) is identical for

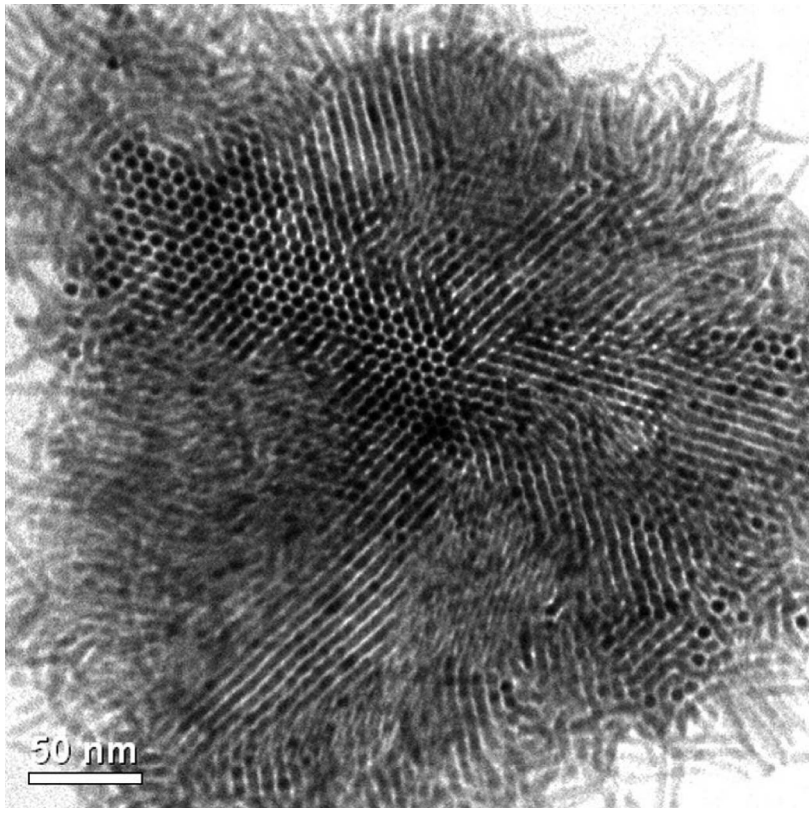


**Figure 5. TEM image of TDPA-, HDA-, and TOP-capped CdS nanorods with concentration of 2.0 wt % (see text for details).**

both cases. Further increase of the concentration of HDA-capped CdS nanorods did not seem helpful for the assembly. Furthermore, upon an increase of the HDA concentration from 1.35 g (used for obtaining Figure 5) to 4.0 g, the percentage of self-bundled CdS nanorods decreased, accompanied by the elongation of CdS nanorods. As a result, types of surfactants should influence the self-assembly. Since a large amount of the TOP was replaced by HDA, the observation of randomly packed bundles suggests that the three octyl groups on the TOP molecule regulate the bundling direction more readily than the single hexadecyl group on the HDA molecule. Moreover, tetradecyl groups on the TDPA might serve as bridges to enhance the corralling structure. Certainly, other minor intrinsic properties of the CdS nanorods, such as the dipole−dipole interaction and van der Waals attraction, might also influence the observed self-assembly. As previously concluded by Korgel and co-workers,[33] side-by-side assembly of CdS nanorods was favored in both dipole−dipole interaction (~470 meV or ~18*kT* at room temperature) and van der Waals attraction (~140 meV or ~5.4*kT*) for CdS with an aspect ratio of 9.9.

As the emission of quantum confined semiconductors is greatly affected by the dimensions of the nanocrystals, luminescent properties of the bundled nanorods might differ from those of nanorods in solution. Curve a of Figure 6 shows emission spectra of CdS nanorods synthesized with TDPA and TOP and dispersed in a toluene solution (0.1 wt %). In comparison, curve b is that of a single-bundled array-deposited thin film and measured by a confocal microscope focused on an array area of 0.5 μm in diameter using a GaN laser (406 nm). Clearly, the intensity of the broad emission band from 525 to 700 nm, which arose from defect states of CdS nanorods in solution, decreased significantly when the nanorods were corralled together. This result was also supported by the corresponding relaxation dynamics, in which the lifetime of the band-edge emission (monitored at 465 nm) of CdS in toluene solution was measured to be 550 ps. On the other hand, probing the area of the CdS self-bundle array with confocal microscope revealed that the lifetime was as long as 4.5 ns, implying the significant suppression of the radiationless quenching processes. Variation of the emission spectra might be due to the great reduction of the lateral surface area in self-bundled arrays. In the CdS bundles, electrons may hop to the neighboring rods, causing the process of recombination at the defect states to be quenched. Supplementary support of this viewpoint is rendered by tuning the GaN laser to the peripheral region (observed with a microscope) of the self-bundle arrays where the assembly is in a relatively loose structure, resulting in an increase in the intensity ratio for CdS *versus* defect emission (*cf.* curve c *versus* curve b). Finally, by redispersing the assembled CdS bundles into toluene, emission of defect states returns to the same magnitude as curve a, demonstrating the physically reversible phenomenon in the self-bundled CdS nanorods.

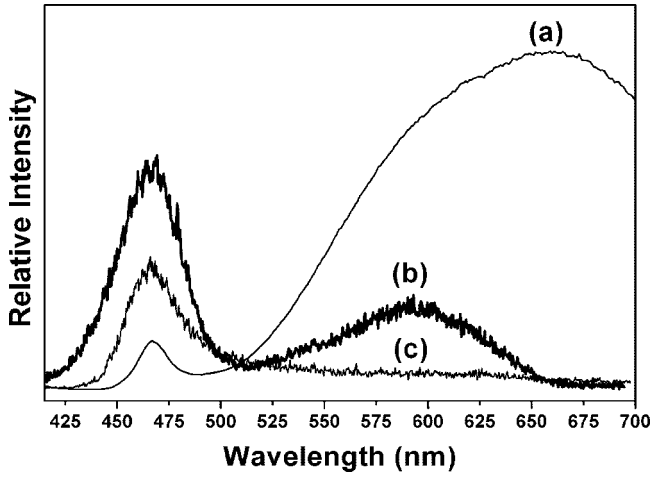


**Figure 6. The normalized emission spectra of (a) CdS nanorods (synthesized by using TDPA and TOP) solution; (b) peripheral and (c) central region of a single array in the deposited thin film measured by a confocal microscope. The excitation wavelength is 406 nm (GaN laser) for all measurements.**

## CONCLUSION

In summary, exclusive self-assemblies of TDPA- and TOP-capped CdS nanorods in the absence of external direction-controlling processes (*e.g.*, external electric field, polymer matrix, or highly oriented pyrolytic carbon) are reported. Combining the results and discussion elaborated above, we thus conclude that by using TDPA and TOP as surfactants, the as-prepared CdS nanorods start to corral together with concentration higher than 2.0% weight percent in toluene. It is believed that the first portion of nanorods, standing normal to the substrate, serves as a nucleation site. Subsequently, the neighboring nanorods tend to assemble in the same direction with the assistance of the hydrocarbon chains on surfactants or the interactions among nanorods. The net result is self-assemblies with outer edges of leaning bundles and an inner part of hexagonal packing perpendicular to the substrate. In comparison to the dominant defect emission of CdS nanorods in toluene solution, the single bundled arrays in a deposited thin film a show dramatic decrease of the defect emission, implying the possibilities of enhancing electron transport between nanorods. Accordingly, on the basis of a simple, straightforward bottom-up solution method, it is feasible to construct a monolayer of nanorod-bundled polarizer with thickness in the dimension of nanometers and area in the dimension of micrometers in an aim to greatly facilitate the future preparation of light-emitting devices.

## EXPERIMENTAL SECTION

Tetradecylphosphonic acid (TDPA, 98%) was purchased from Alfa Aesar. Tri*n*-octylphosphine (TOP, >85% and *n*-hexadecylamine (HDA, 90% were purchased from TCI. Cadmium oxide (CdO, 99.99%) and sulfur (S, 99.5%) powder were obtained from Strem Chemicals and ACROS, respectively. Chemicals were used as received.

CdS nanorods was synthesized according to the literature methods[8] with modification by varying surfactants. Briefly, a sulfur injection solution containing 0.072 g of sulfur (2.25 mmol) was prepared by dissolving sulfur powder in 2 mL of tri-*n*-octylphosphine. A 0.1 g portion of CdO (0.78 mmol) and 0.4565 g of TDPA (1.64 mmol) were loaded into a 50 mL three-neck flask and heated to 200 °C under Ar flow. After the CdO was completely dissolved, judging by the disappearance of the brown color of CdO, the Cd−TDPA complex was allowed to cool to room temperature.

As for the addition of TOP (or HDA), the weight percentage has been optimized such that the formation of the CdS self-bundle array was maximized. In detail, 5 mL of TOP or 1.35 g of HDA was added to the flask, and the temperature was raised to 330 °C to produce an optically clear solution. At this temperature, the sulfur injection solution was swiftly injected into the hot solution. The reaction mixture was maintained at 330 °C for growth of CdS crystals. After 5 min, the temperature was quenched to 40 °C to terminate the reaction. Five mL of toluene was then introduced to dissolve the reaction mixture, and yellow precipitate was obtained by adding 5 mL of isopropanol, and the mixture was centrifuged at 3000 rpm for 5 min. The precipitate was washed with toluene and isopropanol ×3 and redispersed in toluene for the TEM characterization. The dried powder of the precipitate was obtained for the XRD measurement. The shapes and size distributions of the nanocrystals were measured with a JEOL JEM 1230 transmission electron microscope (TEM). The surface energies of suspensions with different CdS concentrations were determined using the pendant-drop method,[35] and the data was analyzed with DataPhysics SCA20 software. The crystal structure and phases of the synthesized samples were analyzed by X-ray powder diffraction (XRD) on a PANalytical X'Pert PRO with Cu Kα X-ray. Emission spectra were recorded with an Edinburgh (FS920) fluorometer. To investigate the possible differences in photoluminescence between nanorods in solution and those in self-assembled bundles, the latter were measured with a confocal microscope (WITec AlphaSNOM) coupled with a red-sensitive charge coupled detector (CCD, Princeton Instruments, PI-MAX). Note that in the confocal microscopy, the probing laser (406 nm, 0.3 μm in diameter) was located on the region of self-assembled bundles determined by TEM. Ti:sapphire laser (Tsunami, Spectra-Physics) with an 80 MHz repetition rate was used as the excitation source for the lifetime measurement. This laser beam (820 nm) was directed into a doubling crystal (BBO) to yield an UV beam (406 nm) as a pulsed excitation source for the solution study. As for the self-bundled CdS nanorods, the 406 nm beam was then guided to a telescope for focusing. The confocal microscope was applied to monitor the self-bundled CdS nanorods in an area of 0.5 μm in diameter. The fluorescence signal was analyzed by the time-correlated single photon counting system (SPC-300, Becker & Hickl) and high speed photodetector module (OT900, Edinburgh).

*Acknowledgment.* We thank the National Science Council, Taiwan (No. NSC 96-2120-M-002-007) for financially supporting this research.

*Supporting Information Available:* Fourier filtered micrograph with enhanced contrast of the same area in Figure 1a and an extended TEM image of self-assembled CdS nanorods synthesized with TDPA and TOP. This material is available free of charge *via* the Internet at http://pubs.acs.org.

## REFERENCES AND NOTES

1. Peng, X. G.; Manna, L.; Yang, W. D.; Wickham, J.; Scher, E.; Kadavanich, A.; Alivisatos, A. P. Shape Control of CdSe Nanocrystals. *Nature* **2000**, *404*, 59–61.
2. Hu, J. T.; Li, L. S.; Yang, W. D.; Manna, L.; Wang, L. W.; Alivisatos, A. P. Linearly Polarized Emission from Colloidal Semiconductor Quantum Rods. *Science* **2001**, *292*, 2060–2063.
3. Talapin, D. V.; Koeppe, R.; Gotzinger, S.; Kornowski, A.; Lupton, J. M.; Rogach, A. L.; Benson, O.; Feldmann, J.; Weller, H. Highly Emissive Colloidal CdSe/CdS Heterostructures of Mixed Dimensionality. *Nano Lett.* **2003**, *3*, 1677–1681.
4. Hikmet, R. A. M.; Chin, P. T. K.; Talapin, D. V.; Weller, H. Polarized-Light-Emitting Quantum-Rod Diodes. *Adv. Mater.* **2005**, *17*, 1436–1439.
5. Acharya, S.; Patla, I.; Kost, J.; Efrima, S.; Golan, V. Switchable Assembly of Ultra Narrow CdS Nanowires and Nanorods. *J. Am. Chem. Soc.* **2006**, *128*, 9294–9295.
6. Manna, L.; Scher, E. C.; Alivisatos, A. P. Synthesis of Soluble and Processable Rod-, Arrow-, Teardrop-, and Tetrapod-Shaped CdSe Nanocrystals. *J. Am. Chem. Soc.* **2000**, *122*, 12700–12706.
7. Peng, Z. A.; Peng, X. G. Mechanisms of the Shape Evolution of CdSe Nanocrystals. *J. Am. Chem. Soc.* **2001**, *123*, 1389–1395.
8. Peng, Z. A.; Peng, X. G. Formation of Highly-Quality CdTe, CdSe, and CdS Nanocrystals Using CdO as Precursor. *J. Am. Chem. Soc.* **2001**, *123*, 183–184.
9. Jun, Y. W.; Lee, S. M.; Kang, N. J.; Cheon, J. W. Controlled Synthesis of Multi-armed CdS Nanorod Architectures Using Monosurfactant System. *J. Am. Chem. Soc.* **2001**, *123*, 5150–5151.

10. Li, L. S.; Hu, J. T.; Yang, W. D.; Alivisatos, A. P. Band Gap Variation of Size- and Shape-Controlled Colloidal CdSe Quantum Rods. *Nano Lett.* **2001**, *1*, 349–351.
11. Qu, L. H.; Peng, Z. A.; Peng, X. G. Alternative Routes toward High Quality CdSe Nanocrystals. *Nano Lett.* **2001**, *1*, 333–337.
12. Qu, L. H.; Peng, X. G. Control of Photoluminescence Properties of CdSe Nanocrystals in Growth. *J. Am. Chem. Soc.* **2002**, *124*, 2049–2055.
13. Peng, Z. A.; Peng, X. G. Nearly Monodisperse and Shape-Controlled CdSe Nanocrystals *via* Alternative Routes: Nucleation and Growth. *J. Am. Chem. Soc.* **2002**, *124*, 3343–3353.
14. Manna, L.; Scher, E. C.; Li, L. S.; Alivisatos, A. P. Epitaxial Growth and Photochemical Annealing of Graded CdS/ZnS Shells on Colloidal CdSe Nanorods. *J. Am. Chem. Soc.* **2002**, *124*, 7136–7145.
15. Yu, W. W.; Peng, X. G. Formation of High-Quality CdS and Other II-VI Semiconductor Nanocrystals in Noncoordinating Solvents: Tunable Reactivity of Monomers. *Angew. Chem., Int. Ed.* **2002**, *41*, 2368–2371.
16. Peng, X. G. Mechanisms for the Shape-Control and Shape-Evolution of Colloidal Semiconductor Nanocrystals. *Adv. Mater.* **2003**, *15*, 459–463.
17. Mokari, T.; Banin, U. Synthesis and Properties of CdSe/ZnS Core/Shell Nanorods. *Chem. Mater.* **2003**, *15*, 3955–3960.
18. Yu, W. W.; Wang, Y. A.; Peng, X. G. Formation and Stability of Size-, Shape-, and Structure-Controlled CdTe Nanocrystals: Ligand Effects on Monomers and Nanocrystals. *Chem. Mater.* **2003**, *15*, 4300–4308.
19. Milliron, D. J.; Hughes, S. M.; Cui, Y.; Manna, L.; Li, J.; Wang, L. W.; Alivisatos, A. P. Colloidal Nanocrystal Heterostructures with Linear and Branched Topology. *Nature* **2004**, *430*, 190–195.
20. Qu, L. H.; Yu, W. W.; Peng, X. G. In Situ Observation of the Nucleation and Growth of CdSe Nanocrystals. *Nano Lett.* **2004**, *4*, 465–469.
21. Shieh, F.; Saunders, A. E.; Korgel, B. A. General Shape Control of Colloidal CdS, CdSe, CdTe Quantum Rods and Quantum Rod Heterostructures. *J. Phys. Chem. B* **2005**, *109*, 8538–8542.
22. Kumar, S.; Nann, T. Shape Control of II-VI Semiconductor Nanomaterials. *Small* **2006**, *2*, 316–329.
23. Gur, I.; Fromer, N. A.; Geier, M. L.; Alivisatos, A. P. Air-Stable All-Inorganic Nanocrystal Solar Cells Processed from Solution. *Science* **2005**, *310*, 462–464.
24. Huynh, W. U.; Dittmer, J. J.; Alivisatos, A. P. Hybrid Nanorod-Polymer Solar Cells. *Science* **2002**, *295*, 2425–2427.
25. Qnsager, L. The Effects of Shape on the Interaction of Colloidal Particles. *Ann. N. Y. Sci.* **1949**, *51*, 627–659.
26. Li, L. S.; Walda, J.; Manna, L.; Alivisatos, A. P. Semiconductor Nanorod Liquid Crystals. *Nano Lett.* **2002**, *2*, 557–560.
27. Li, L. S.; Alivisatos, A. P. Semiconductor Nanorod Liquid Crystals and Their Assembly on a Substrate. *Adv. Mater.* **2003**, *15*, 408–411.
28. Talapin, D. V.; Shevchenko, E. V.; Mirry, C. B.; Kornowski, A; Forster, S.; Weller, H. CdSe and CdSe/CdS Nanorod Solids. *J. Am. Chem. Soc.* **2004**, *126*, 12984–12988.
29. Ryan, K. M.; Mastroianni, A.; Stancil, K. A.; Liu, H. T; Alivisatos, A. P. Electric-Field-Assisted Assembly of Perpendicularly Oriented Nanorod Superlattices. *Nano Lett.* **2006**, *6*, 1479–1482.
30. Gupta, S.; Zhang, Q. L.; Emrick, T.; Russell, T. P. "Self-Corralling" Nanorods under an Applied Electric Field. *Nano Lett.* **2006**, *6*, 2066–2069.
31. Ahmed, S.; Ryan, K. M. Self-Assembly of Vertically Aligned nanorod Supercrystals Using Highly Oriented Pyrolytic Graphite. *Nano Lett.* **2007**, *7*, 2480–2485.
32. Carbone, L.; Nobile, C.; Giorgi, M. D.; Sala, F. D.; Morello, G. Pompa, P.; Hytch, M.; Snoeck, E.; Fiore, A.; Franchini, I. R.; *et al*. Synthesis and Micrometer-Scale Assembly of Colloidal CdSe/CdS Nanorods Prepared by a Seeded Growth Approach. *Nano Lett.* **2007**, *7*, 2942–2950.
33. Ghezelbash, A.; Koo, B.; Korgel, B. A. Self-Assembled Stripe Patterns of CdS Nanorods. *Nano Lett.* **2006**, *6*, 1832–1836.
34. He, J.; Zhang, Q. L.; Gupta, S; Emrick, T.; Russell, T. P.; Thiyagarajan, P. Drying Droplets: A Window into the Behavior of Nanorods at Interface. *Small* **2007**, *3*, 1214–1217.
35. Winkel, D. Theoretical Refinement of the Pendant Drop Method for Measuring Surface Tensions. *J. Phys. Chem.* **1965**, *69*, 348–350.
36. Wishnia, A. The Hydrophobic Contribution to Micelle Formation: The Solubility of Ethane, Propane, Butane, and Pentane in Sodium Dodecyl Sulfate Solution. *J. Phys. Chem.* **1963**, *67*, 2079–2082.
37. Bent, S. F. The Hydrophobic Contribution to Micelle Formation: The Solubility of Ethane, Propane, Butane, and Pentane in Sodium Dodecyl Sulfate Solution. *ACS Nano* **2007**, *1*, 10–12.